Reflectometry Observation Of Density Fluctuations Associated With The Resonant q = 2 Surface In WENDELSTEIN VII-AS Stellarator

J. Sanchez#, H.J. Hartfuß, WVII-AS Team, NBI Team, Pellet Injection Team

Max-Planck-Institut für Plasmaphysik
EURATOM Ass., 8046 Garching, FRG

E. Anabitarte, A.P. Navarro

Association EURATOM/CIEMAT, 28040 Madrid, Spain

ECRH Group

Institut für Plasmaforschung der Universität Stuttgart
7000 Stuttgart, FRG

MAX-PLANCK-INSTITUT FÜR PLASMAPHYSIK

8046 GARCHING BEI MÜNCHEN

MAX-PLANCK-INSTITUT FÜR PLASMAPHYSIK

GARCHING BEI MÜNCHEN

Reflectometry Observation Of Density Fluctuations Associated With The Resonant q = 2 Surface In WENDELSTEIN VII-AS Stellarator

J. Sanchez#, H.J. Hartfuß, WVII-AS Team, NBI Team, Pellet Injection Team

Max-Planck-Institut für Plasmaphysik
EURATOM Ass., 8046 Garching, FRG

E. Anabitarte, A.P. Navarro

Association EURATOM/CIEMAT, 28040 Madrid, Spain

ECRH Group

Institut für Plasmaforschung der Universität Stuttgart
7000 Stuttgart, FRG

Die nachstehende Arbeit wurde im Rahmen des Vertrages zwischen dem Max-Planck-Institut für Plasmaphysik und der Europäischen Atomgemeinschaft über die Zusammenarbeit auf dem Gebiete der Plasmaphysik durchgeführt.

on leave from Association EURATOM/CIEMAT, 28040 Madrid, Spain

WVII-AS Team:

R. Brakel, R. Burhenn, G. Cattanei, A. Dohdy, D. Dorst, A. Elsner,
K. Engelhardt, V. Erckmann, D. Evans, U. Gasparino, G. Grieger,
P. Grigull, H. Hacker, H.J. Hartfuß, H. Jäckel, R. Jaenicke,
J. Junker, M. Kick, H. Kroiss, G. Kühner, I. Lakicevic,
H. Maaßberg, C. Mahn, W. Ohlendorf, H. Renner, H. Ringler, J. Saffert
F. Sardei, M. Tutter, A. Weller, E. Würsching, M. Zippe.

NBI Team

J.H. Feist, K. Freudenberger, R.C. Kunze, W. Ott, F.-P. Penningsfeld, E. Speth,

Pellet Injection Group

K. Büchl, R. Lang

ECRH Group

W. Kasparek, G.A. Müller, P.G. Schüller, M. Thumm

Abstract

Enhanced density fluctuations associated with the rational q = 2 ($\iota = 0.5$) surface have been observed by a microwave reflectometer in currentless NBI heated discharges with pellet injection at an edge iota of 0.52. Radial scan of MHD activity locates coherent density fluctuations at r/a = 0.7. Frequency and amplitude are estimated.

Correlation between the level of the local density turbulence and the iota value during iota modulation at 300 Hz leads to the conclusion that local enhancement of the broadband density turbulence exists at the points where the rational iota values are crossed. A phase jump in the turbulence modulation occurs for r/a = 0.7, indicating the location of the resonant $\iota = 0.5$ surface.

The effect can be the basis of a new method to analyze the evolution of the iota profile inside the plasma with interesting applications in current control experiments.

1. Introduction

The nearly shearless modular stellarator WENDELSTEIN VII-AS
(R = 2 m, $\overline{a}$ = 0.2 m) started plasma operation in october 1988. [1] So far ECH experiments at B = 1.25 and 2.5 T as well as NBI experiments at B = 1.25 T have been conducted. As observed in the former WENDELSTEIN VII-A machine too [2], a strong correlation between the confinement properties and the rotational transform iota has been found [3]. Reduced confinement was observed for the low order rational values. In addition poor confinement is found at the values 5/m where the "natural resonances" due to the five fold symmetry of the machine are present. In the vicinity of the low order rational surfaces (1/2 and 1/3) best confinement is observed.

Optimum confinement is obtained in the low shear configuration if the "resonant" iota

values can be excluded from the plasma column. The close proximity of optimum and minimum confinement values makes current control necessary under plasma operation, because the iota profile inside the plasma is affected by toroidal currents and beta effects. Although the global net current can be kept at zero level using a small OH induced current opposed to the gradient driven bootstrap current, the different currents flow at different radial positions affecting the iota profile.

Additional tools for configuration control inside the plasma are vertical fields and the currents driven by the NBI and most promising the ECH heating systems. In this context experimental information on the iota profile is highly needed.

Since the currents involved are very small ($\leq$ 5 kA), the methods used in tokamaks i.e. polarimetry can hardly be adapted here. The search for rational surfaces with the associated MHD fluctuations has been used so far in addition to the information of magnetic coil diagnostics with the lack of spatial resolution. The location of temperature perturbations in discharges with OH currents have been achieved by using the Thomson diagnostic synchronized with the Mirnov coils [5] and soft X-ray tomography [6]. In the case of currentless discharges, density and temperature fluctuations associated with the q = 1 surface have been observed [7]. The situation becomes more difficult when the q = 1 surface is not included in the plasma, which is the case in WENDELSTEIN VII-AS.

In this paper we report the observation of configurational effects in the plasma edge ($r/a \geq 0.6$) by the use of microwave reflectometry which is sensitive to density fluctuations through induced movements in the reflecting layer.

A radial scan of coherent perturbations gives the position of magnetic islands with good resolution. In addition a dependence of the local broadband density turbulence level on the local iota value has been observed with the reflectometer in discharges with iota modulation at 300 Hz. This effect also leads to the location of the resonant surfaces in the plasma even if no well defined MHD activity is present. The slope (positive or negative) of the iota profile in the vicinity of the rational value can also be determined.

Crosscorrelation of the reflectometer and the iota signals are also a powerful tool to analyze skin times at different radial positions in the plasma edge and their possible relation to the resistivity in this region where anomalous transport is dominant.

2. Reflectometry

Microwave reflectometry is based on the reflection of microwave radiation in the millimeter range at the plasma cutoff layer. The phase delay between the launched and the reflected waves gives information on the location and the movement of the reflecting layer [8-12].

Wheras microwave scattering measurements are only sensitive to perturbations with a given wavenumber **k** (the Bragg condition must be fulfilled), reflectometry gives a **k** integrated measurement, mainly sensitive to the low **k** perturbations since the wavelength of the incident microwave radiation must be smaller than that of the density perturbation. Those low **k** perturbations are very important because they involve most of the fluctuation power and can only be measured in scattering experiments with poor spatial

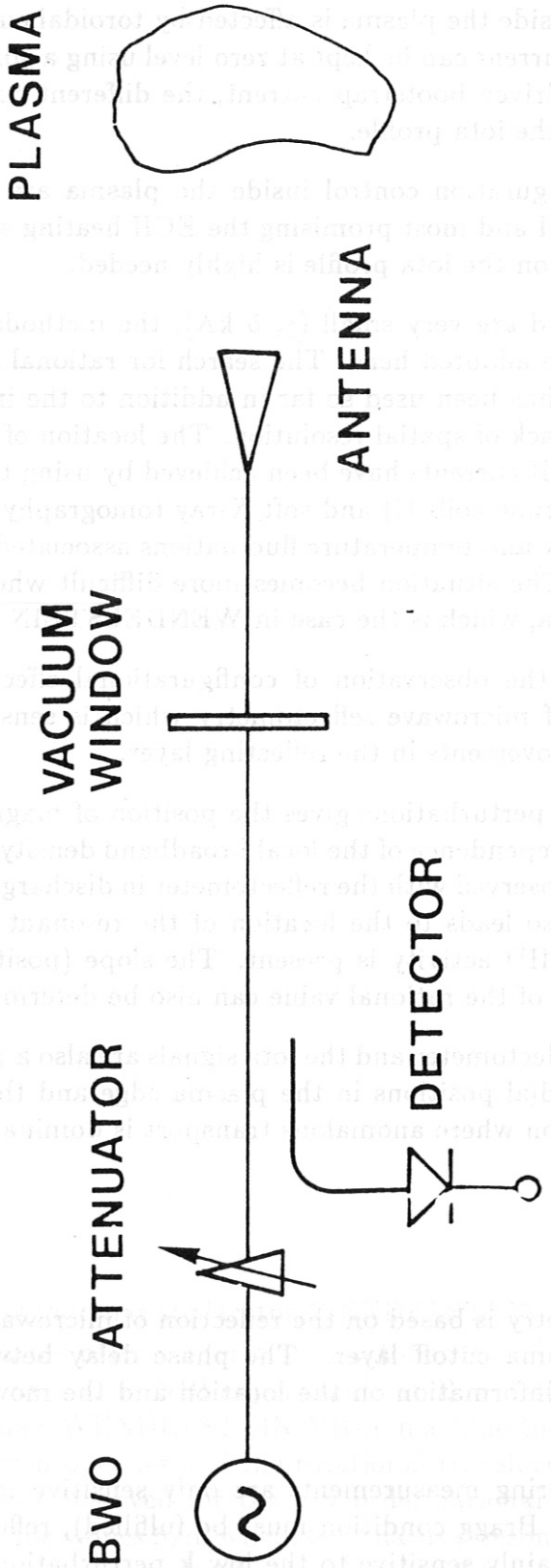

Fig.1. General scheme of the single antenna homodyne reflectometer

resolution [13]. MHD modes are found in this wavenumber range.

The use of electronically tunable oscillators in reflectometry allows to probe radially different reflecting points. Spatial resolution is achieved since the refraction index for the microwave beam is much more sensitive to density variations when the beam frequency approaches the cutoff frequency. This means that the phase delay due to local density perturbation along the propagation path of the beam becomes strongly enhanced when the perturbation is located at the reflecting layer. Line integrated effects are very small.

As the simplest approach a homodyne receiver has been used (fig.1). The microwave beam is launched and received by using the same antenna. The wave reflected at the plasma and that reflected at some reference (usually the vacuum window) are mixed in a square law detector diode.The output voltage at the detector will be:

$$v(t) = p_0 + p_1 + 2\sqrt{p_0 p_1}\cos[\delta(t)] \tag{1}$$

p_0 is the power coming from the reference, p_1 that one coming from reflection at the plasma cutoff layer and $\delta(t)$ is the phase delay of interest.

Usually p_1 is much smaller than p_0. The variation in the output of the diode responds to changes both in the phase δ and in the amplitude p_1 of the signal coupled from the plasma. If no coherent MHD activity is present, $v(t)$ shows a broadband spectrum. When a density fluctuation with a well defined frequency Ω exists, the reflecting layer will have an oscillating movement too. So the phase shift can be written as:

$$\delta(t) = \delta_0 + \Delta\Phi \sin \Omega t$$

and the output voltage at the diode as:

$$v(t) = p_0 + p_1 + 2\sqrt{p_0 p_1}\cos[\delta_0 + \Delta\Phi \sin \Omega t]$$

$v(t)$ can be expressed as an expansion on Bessel functions with argument $\Delta\Phi$

$$v(t) = p_0 + p_1 + 2\sqrt{p_0 p_1}[cos\delta_0[J_0(\Delta\Phi) + 2\sum_k J_{2k}(\Delta\Phi)cos(2k\Omega t)] \tag{2}$$

$$-2sin\delta_0 \sum_k J_{2k+1}(\Delta\Phi)sin(2k+1)\Omega t)]$$

Thus the amplitude spectrum of the recorded signal shows harmonics of the density fluctuation frequency Ω. The number of harmonics with significant amplitude is the higher the bigger $\Delta\Phi$ is. An analysis of the ratio of amplitudes for the harmonics of the same parity leads to an exact determination of $\Delta\Phi$.

Under these conditions a radial scan using different probing frequencies can be carried out, the amplitude of the perturbation at the corresponding different radial positions can be compared.

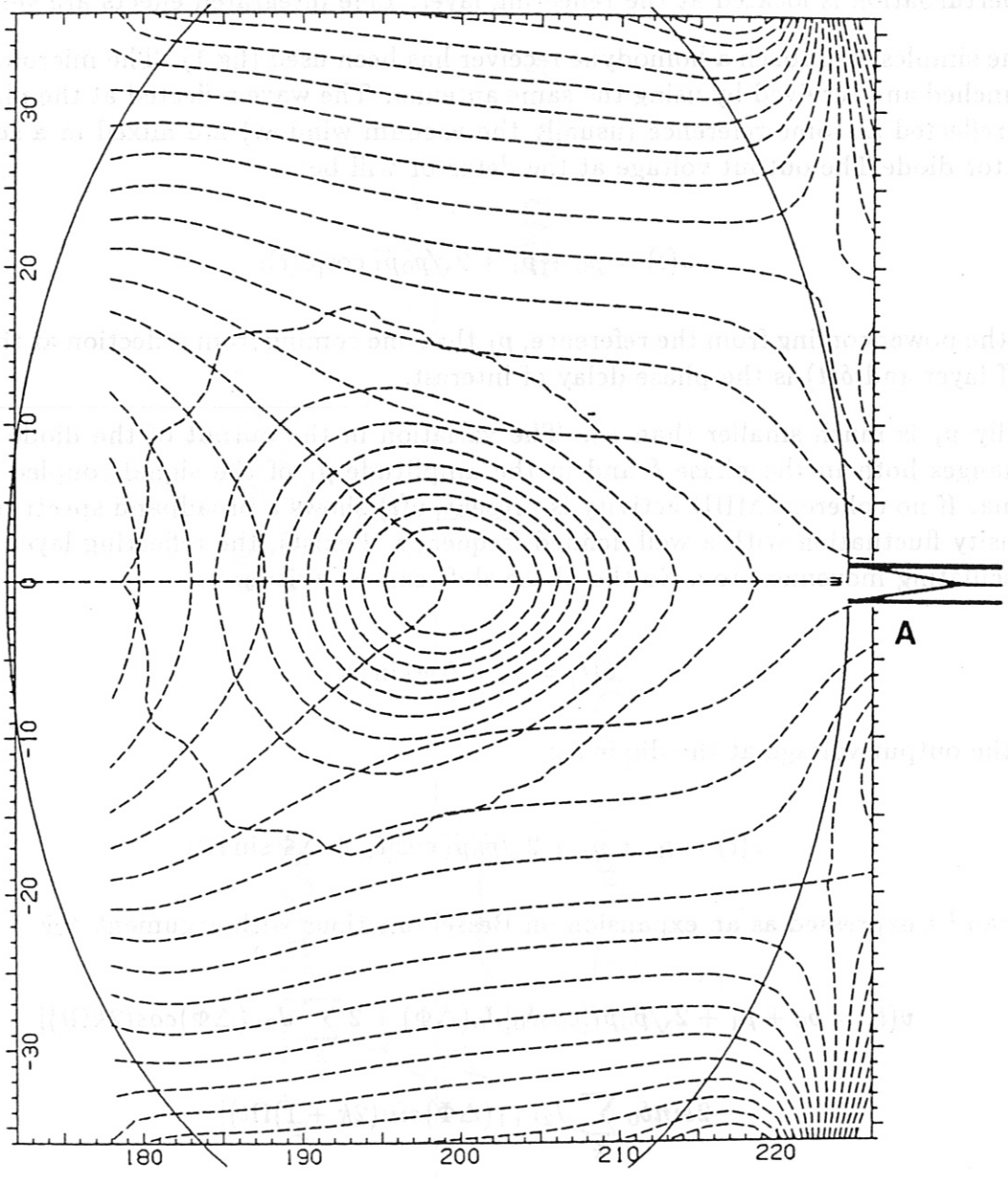

Fig.2. Geometry of antenna A and plasma in the "triangular plane" of WENDELSTEIN VII-AS. The coordinates are given in cm. The flux surfaces correspond to $\iota(a) = 0.47$. B = constant lines are shown, $\Delta B = 250$ G.

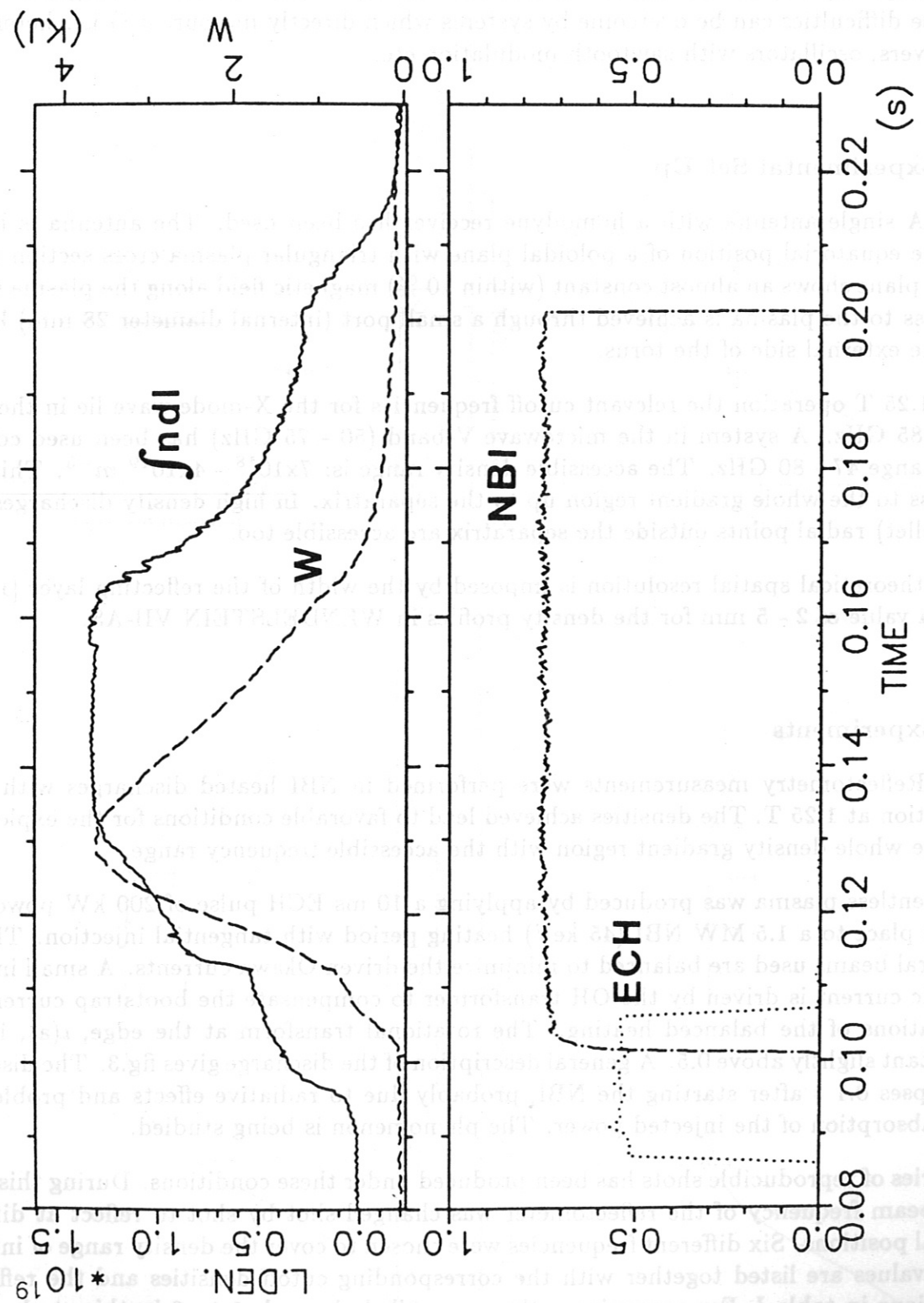

Fig.3. Global parameters of the reproducible discharge. Upper frame: line integrated density (solid line), diamagnetic energy W (dashed line). Lower frame: ECH injected power (point line, full scale = 400 kW), NBI injected power (point dashed line, full scale = 2 MW).

If only broadband turbulence is observed, the radial scan becomes more difficult since p_0 and p_1 usually strongly depend on frequency due to the oscillator used (BWO) and the frequency dependent transmission of the vacuum window and the waveguide system. These difficulties can be overcome by systems which directly measure $\delta(t)$ i.e. heterodyne receivers, oscillators with sawtooth modulation etc.

3. Experimental Set Up

A single antenna with a homodyne receiver has been used. The antenna is located in the equatorial position of a poloidal plane with triangular plasma cross section (fig.2). This plane shows an almost constant (within 10 %) magnetic field along the plasma radius. Access to the plasma is achieved through a small port (internal diameter 28 mm) located at the external side of the torus.

For 1.25 T operation the relevant cutoff frequencies for the X-mode wave lie in the range 40 - 85 GHz. A system in the microwave V-band (50 - 75 GHz) has been used covering the range 47 - 80 GHz. The accessible density range is: $7\text{x}10^{18}$ - $4\text{x}10^{19}$ m^{-3}. This gives access to the whole gradient region up to the separatrix. In high density discharges (NBI + pellet) radial points outside the separatrix are accessible too.

The theoretical spatial resolution is imposed by the width of the reflecting layer [14] and has a value of 2 - 5 mm for the density profiles in WENDELSTEIN VII-AS.

4. Experiments

Reflectometry measurements were performed in NBI heated discharges with pellet injection at 1.25 T. The densities achieved lead to favorable conditions for the exploration of the whole density gradient region with the accessible frequency range.

Currentless plasma was produced by applying a 10 ms ECH pulse of 200 kW power that gives place to a 1.5 MW NBI (45 keV) heating period with tangential injection. The two neutral beams used are balanced to minimize the driven Okawa currents. A small induced ohmic current is driven by the OH transformer to compensate the bootstrap current and deviations of the balanced heating. The rotational transform at the edge, ι(a), is kept constant slightly above 0.5. A general description of the discharge gives fig.3. The discharge collapses 0.1 s after starting the NBI, probably due to radiative effects and problems in the absorption of the injected power. The phenomenon is being studied.

A series of reproducible shots has been produced under these conditions. During this series the beam frequency of the reflectometer was changed shot by shot to reflect at different radial positions. Six different frequencies were chosen to cover the density range of interest. The values are listed together with the corresponding cutoff densities and the reflection positions in table I. For convenience they are called channels 1 to 6 in this study, being channel 1 the outermost one.

Electron density and temperature profiles have been measured by Thomson scattering at 0.12 and 0.128 s (fig.4). The reflection points for 0.122 s were determined by linear

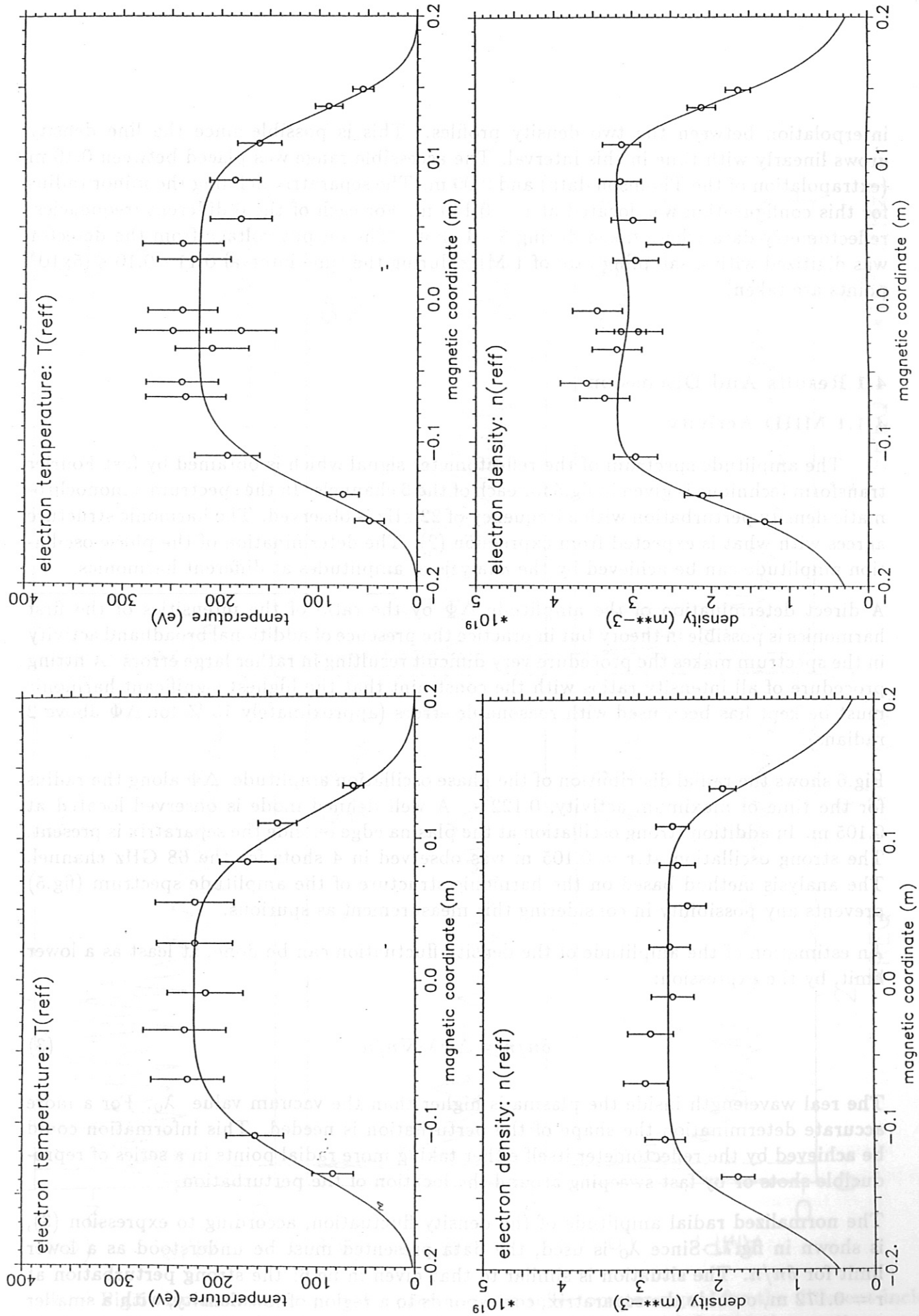

Fig.4. Temperature and density profiles as measured by Thomson scattering, taken at times 0.12 and 0.128 s respectively.

interpolation between the two density profiles. This is possible since the line density grows linearly with time in this interval. The accessible range was placed between 0.19 m (extrapolation of the Thomson data) and 0.09 m. The separatrix defining the minor radius for this configuration was located at r = 0.149 m. For each of the 6 different frequencies, reflectometry data where taken during 3 - 4 shots. The output voltage from the detector was digitized with a sampling rate of 1 MHz during the time interval 0.11 - 0.16 s ($5x10^4$ points are taken).

4.1 Results And Discussion

4.1.1 MHD Activity

The amplitude spectrum of the reflectometer signal which is obtained by fast Fourier transform technique is given in fig.5 for each of the 6 channels. In the spectrum a monochromatic density perturbation with a frequency of 22 kHz is observed. The harmonic structure agrees with what is expected from expression (2). The determination of the phase oscillation amplitude can be achieved by the analysis of amplitudes at different harmonics.

A direct determination of the amplitude $\Delta\Phi$ by the ratio of the intensities of the first harmonics is possible in theory but in practice the presence of additional broadband activity in the spectrum makes the procedure very difficult resulting in rather large errors. A fitting procedure of all intensity ratios with the constraint that the highest significant harmonic must be kept has been used with reasonable errors (approximately 15 % for $\Delta\Phi$ above 2 radians).

Fig.6 shows the radial distribution of the phase oscillation amplitude $\Delta\Phi$ along the radius for the time of maximum activity, 0.122 s. A well defined mode is observed located at 0.105 m. In addition strong oscillation at the plasma edge outside the separatrix is present. The strong oscillation at r = 0.105 m was observed in 4 shots for the 68 GHz channel. The analysis method based on the harmonic structure of the amplitude spectrum (fig.5) prevents any possibility in considering this measurement as spurious.

An estimation of the amplitude of the density fluctuation can be done, at least as a lower limit, by the expression:

$$\delta n/n = \Delta\Phi\lambda_0\nabla n/n \qquad (3)$$

The real wavelength inside the plasma is higher than the vacuum value λ_0. For a more accurate determination the shape of the perturbation is needed. This information could be achieved by the reflectometer itself either taking more radial points in a series of reproducible shots or by fast sweeping around the location of the perturbation.

The normalized radial amplitude of the density fluctuation, according to expression (3), is shown in fig.7. Since λ_0 is used, the data presented must be understood as a lower limit for $\delta n/n$. The situation is similar to that given in fig.6: the strong perturbation at r = 0.172 m, outside the separatrix, corresponds to a region of low density, with a smaller gradient and high sensitivity to any activity in the plasma bulk. Although the analysis of perturbations outside the separatrix and its relation to the internal perturbations is an

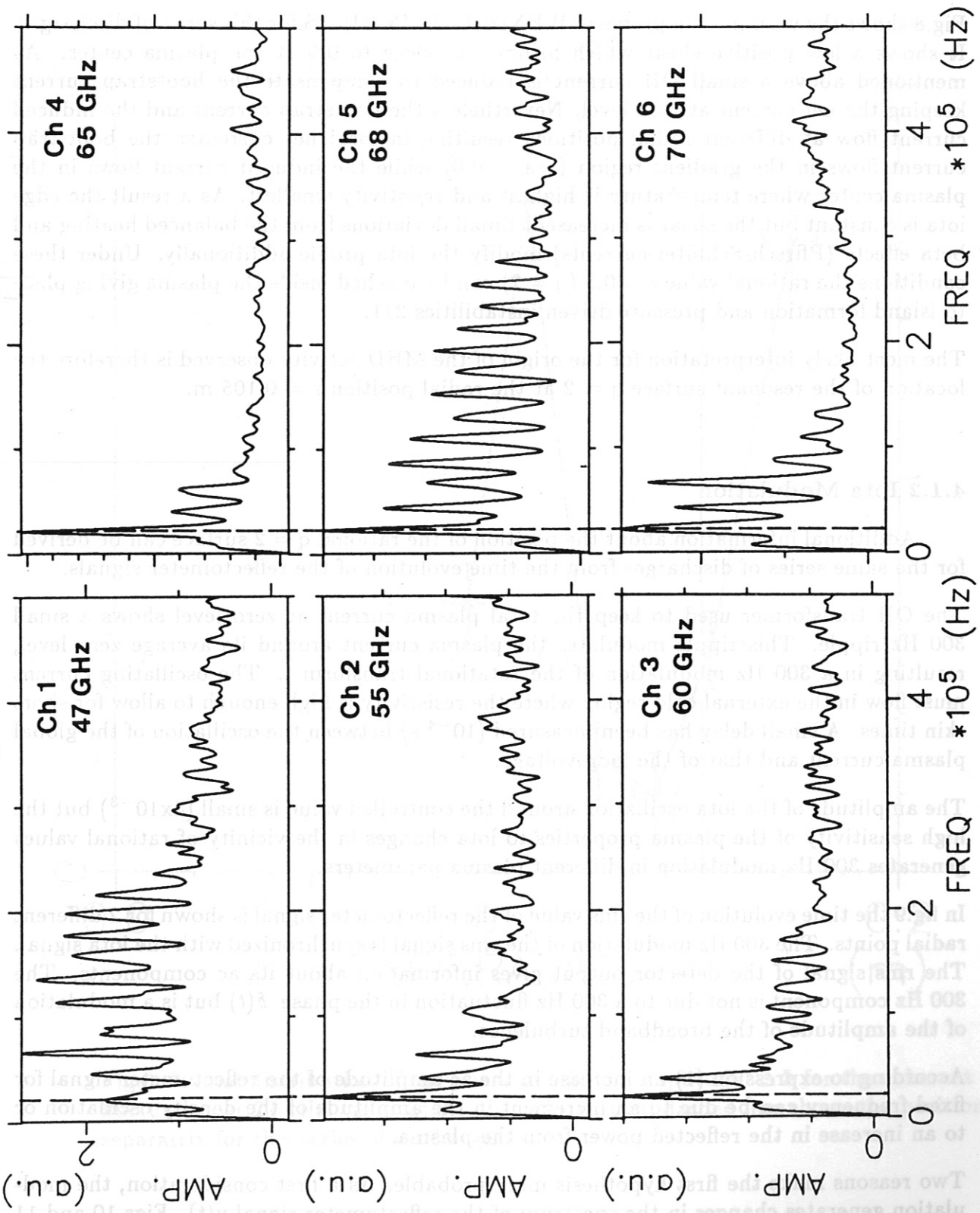

Fig.5. Normalized amplitude spectra of the reflectometer signal for the different incident frequencies showing a dominant perturbation at 22 kHz with harmonic structure at time 0.122 s. The reflection points are listed in table I.

attractive research issue, we only concentrate on the internal instability at r = 0.105 m and its configurational implications.

Fig.8 shows the vacuum iota profile of WENDELSTEIN VII-AS for this series of discharges. It shows a low positive shear which brings iota close to 0.5 at the plasma center. As mentioned above a small OH current is induced to compensate the bootstrap current keeping the net current at zero level. Nevertheless the bootstrap current and the induced current flow at different radial positions resulting in local net currents: the bootstrap current flows in the gradient region (r/a = 0.6) while the induced current flows in the plasma center where temperature is highest and resistivity smallest. As a result the edge iota is constant but the shear is increased. Small deviations from the balanced heating and beta effects (Pfirsch-Schlüter-currents) modify the iota profile additionally. Under these conditions the rational value $\iota = 0.5$ (q = 2) can be reached inside the plasma giving place to island formation and pressure driven instabilities 2/1.

The most likely interpretation for the origin of the MHD activity observed is therefore the location of the resonant surface q = 2 at the radial position r = 0.105 m.

4.1.2 Iota Modulation

Additional information about the position of the rational q = 2 surface can be derived for the same series of discharges from the time evolution of the reflectometer signals.

The OH transformer used to keep the total plasma current at zero level shows a small 300 Hz ripple. This ripple modulates the plasma current around its average zero level, resulting in a 300 Hz modulation of the rotational transform ι. The oscillating current must flow in the external cold region where the resistivity is high enough to allow for short skin times. A small delay has been measured (10^{-4} s) between the oscillation of the global plasma current and that of the loop voltage.

The amplitude of the iota oscillation around the controlled value is small ($4x10^{-3}$) but the high sensitivity of the plasma properties to iota changes in the vicinity of rational values generates 300 Hz modulation in different plasma parameters.

In fig.9 the time evolution of the rms value of the reflectometer signal is shown for 2 different radial points. The 300 Hz modulation of the rms signal is synchronized with the iota signal. The rms signal of the detector output gives information about its ac components. The 300 Hz component is not due to a 300 Hz fluctuation in the phase $\delta(t)$ but is a modulation of the amplitude of the broadband turbulence.

According to expression (1) an increase in the ac amplitude of the reflectometer signal for fixed frequency can be due to an increment in the amplitude of the density oscillation or to an increase in the reflected power from the plasma.

Two reasons make the first hypothesis more probable. As a first consideration, the modulation generates changes in the spectrum of the reflectometer signal v(t). Figs.10 and 11 show how the low ($f \leq 100$ kHz) and the high (250 kHz $\leq f \leq 500$ kHz) frequency components respond in a different way to the iota modulation. In channel 1 mainly the low frequency components are modulated. Moving to deeper radial positions (increasing channel num-

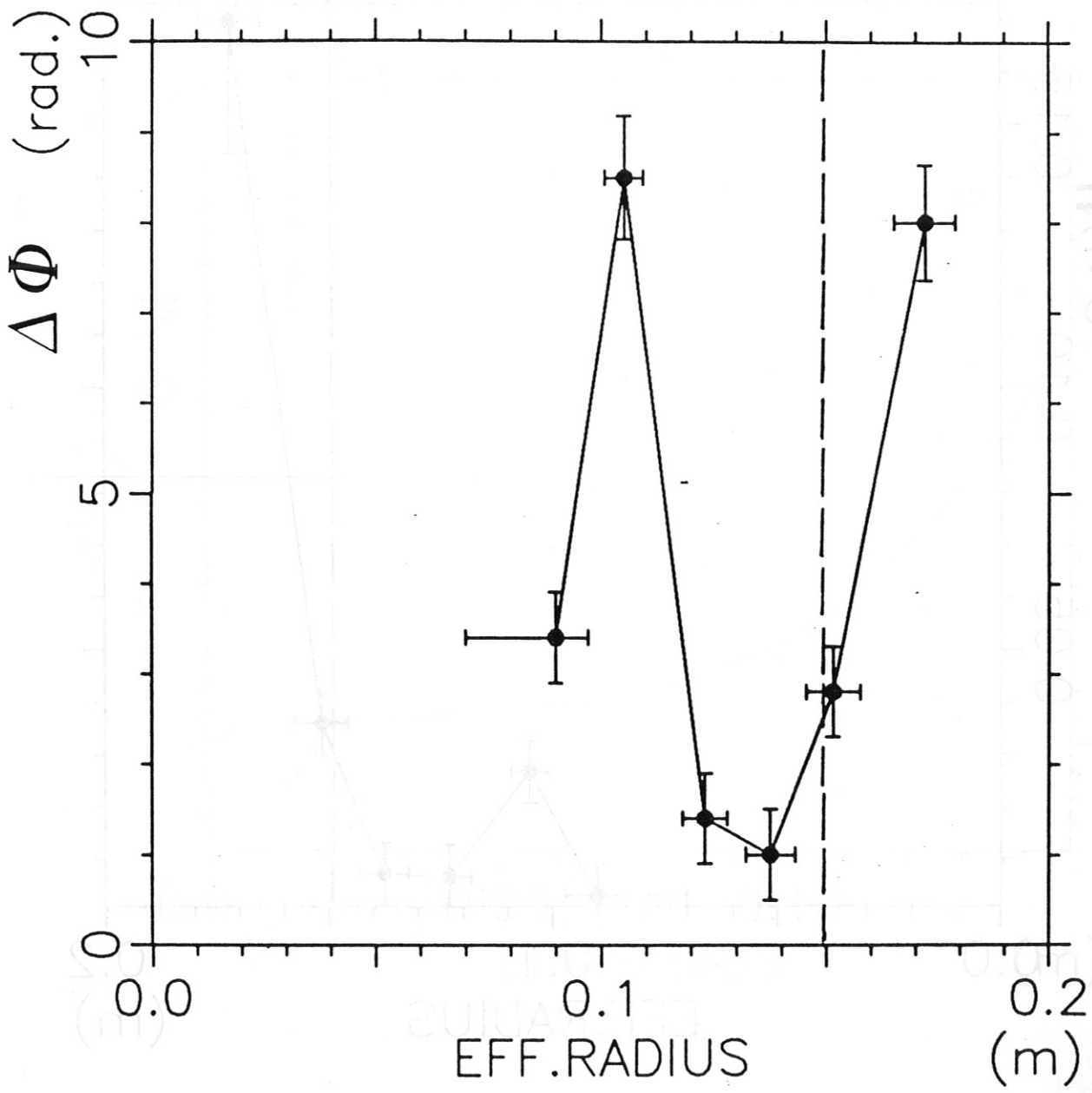

Fig.6. Radial distribution of the phase oscillation amplitude $\Delta\Phi$ for the coherent fluctuation at 22 kHz, taken at 0.122 s. The vertical dashed line shows the position of the separatrix for this series of discharges.

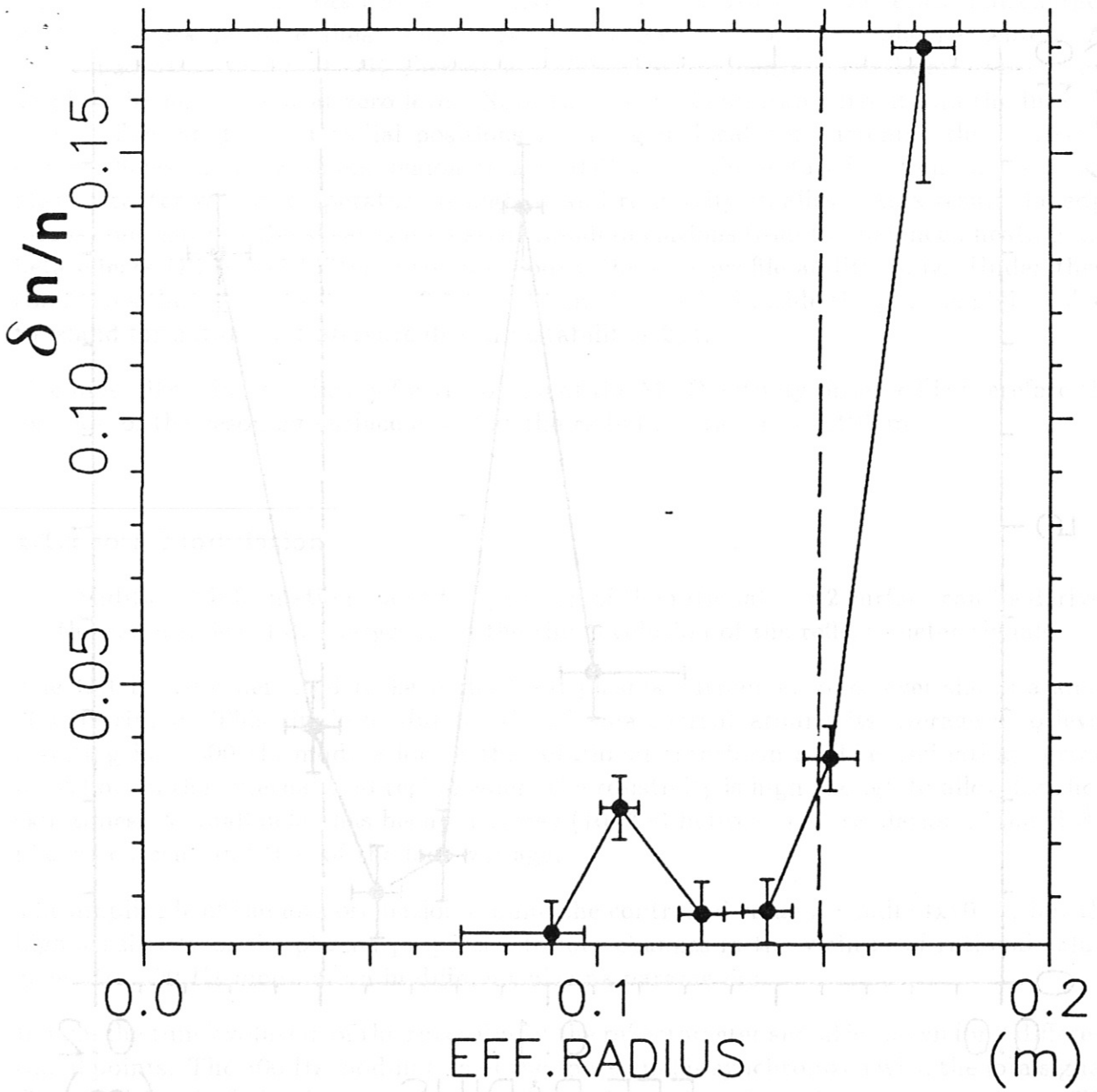

Fig.7. Radial distribution of the relative density fluctuation amplitude for the coherent mode at 22 kHz (0.122 s).Vertical dashed line: position of the separatrix. The amplitude given is a lower limit.

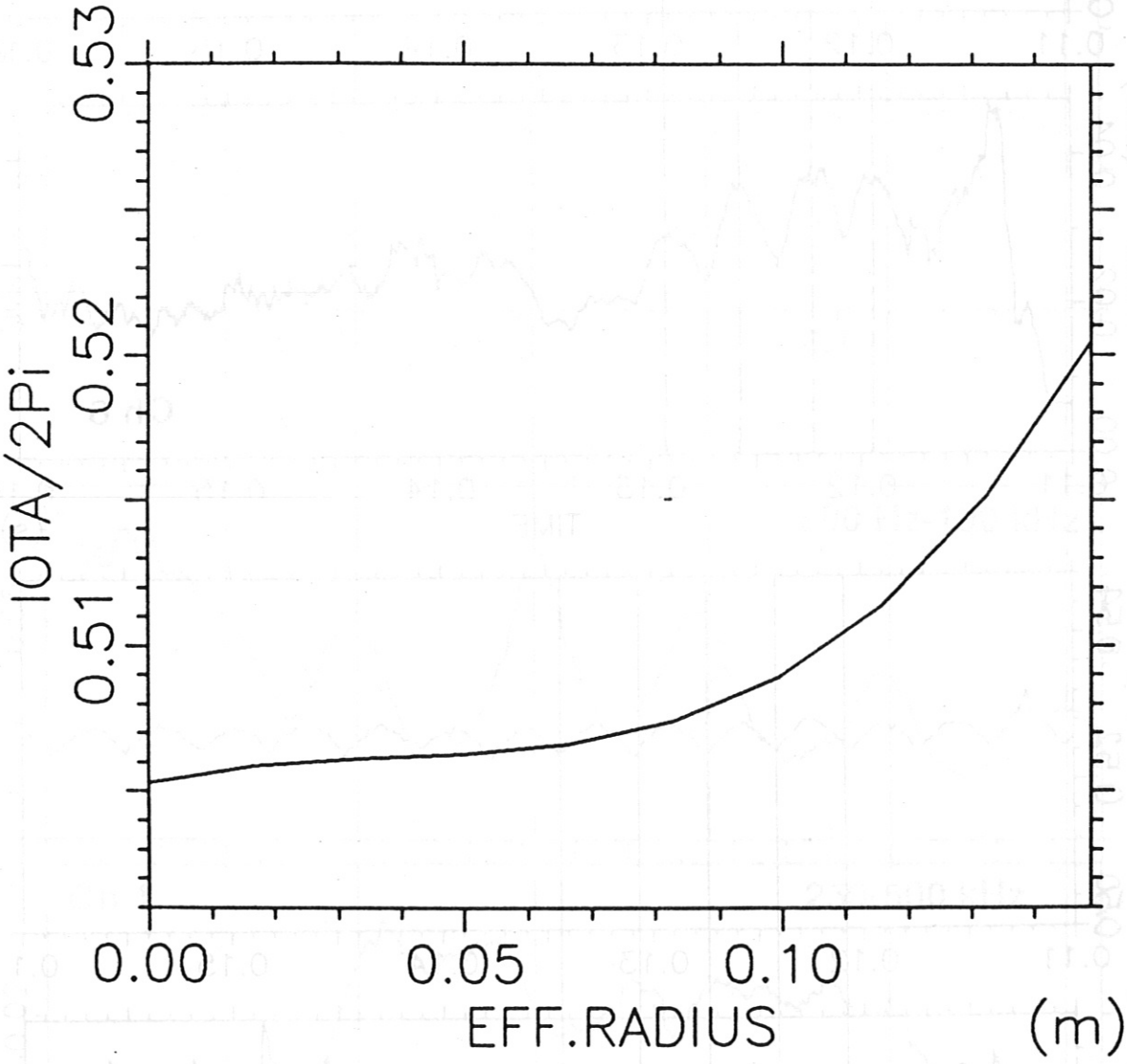

Fig.8. Radial profile of the rotational transform ι for the series of discharges analyzed. A low psitive shear exists.

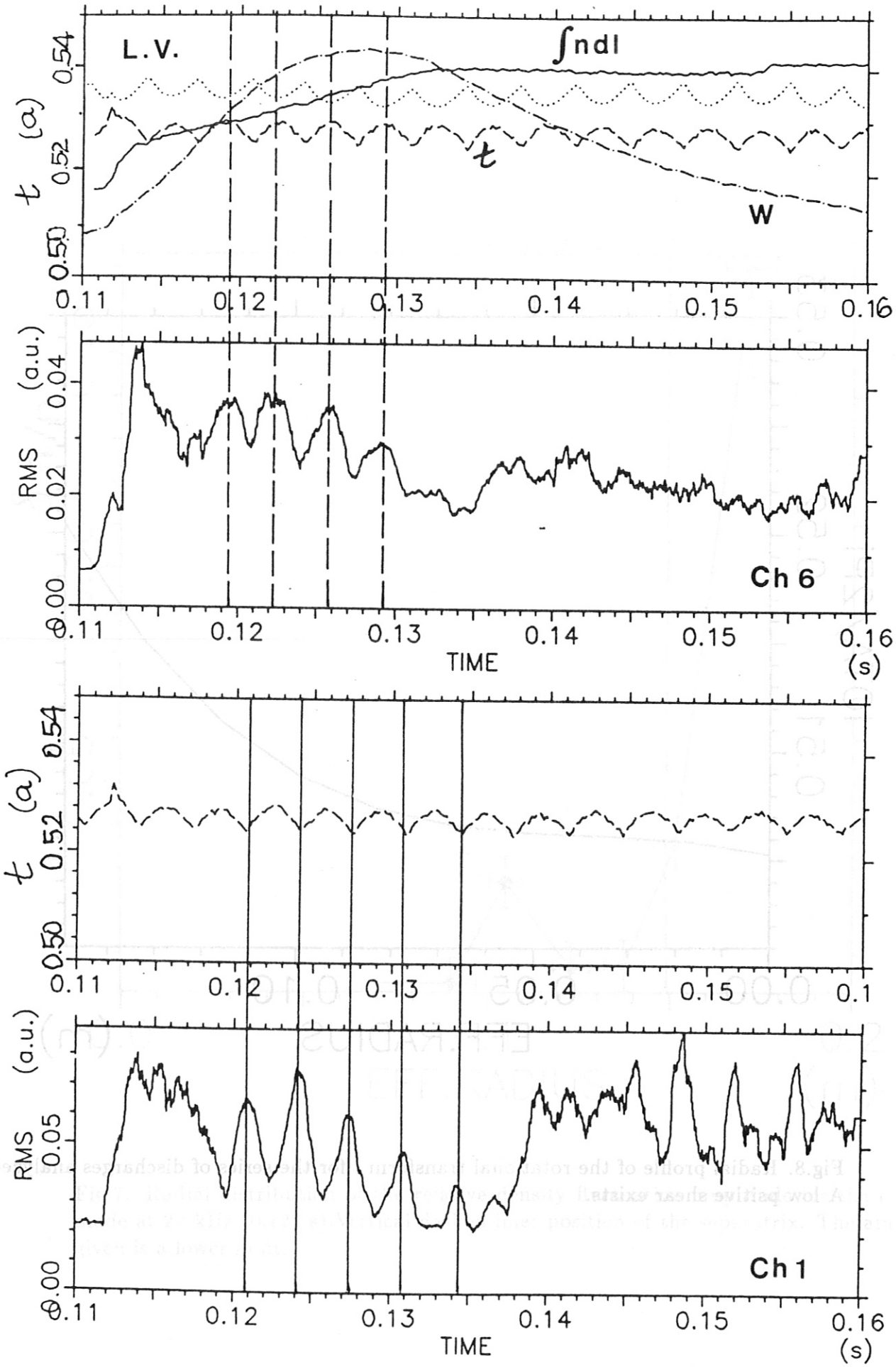

Fig.9. Modulation of the rms reflectometer signal and synchronization with the iota modulation. Upper frame: innermost channel, probing frequency 70 GHz, cutoff frequency $3x10^{19}$ m^{-3} (solid line: line density, dashed line: diamagnetic energy, point line: loop voltage, point-dashed line: edge iota). Lower frame: outermost channel, probing frequency 47 GHz, cut off frequency $7x10^{18}$ m^{-3}.

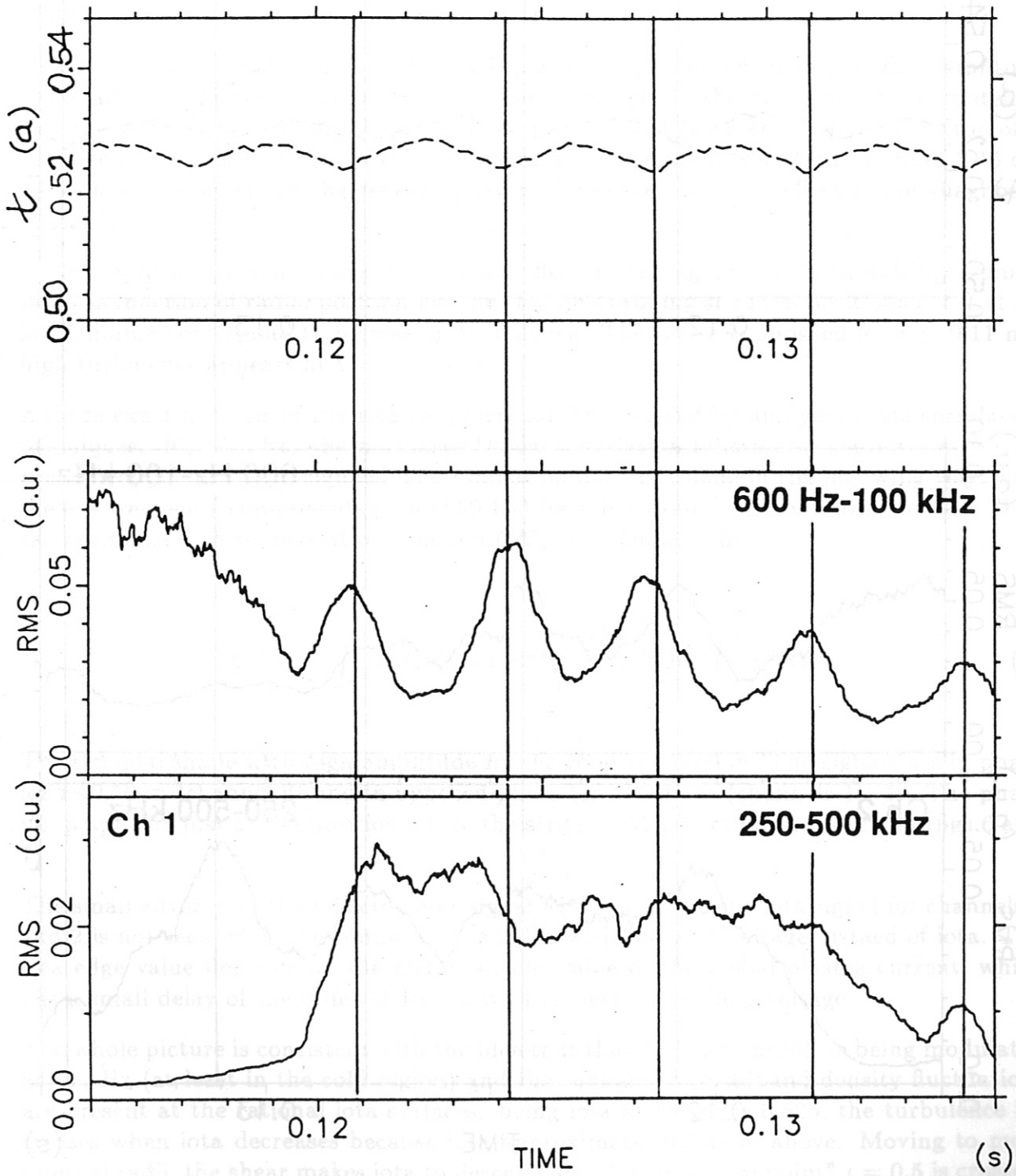

Fig.10. Different behaviour of the modulation when the low and high frequency components of the density turbulence are selected. Channel 1, f = 47 GHz. Upper frame: low frequency components, 600 Hz - 100kHz. Lower frame: high frequency components, 250 - 500 kHz.

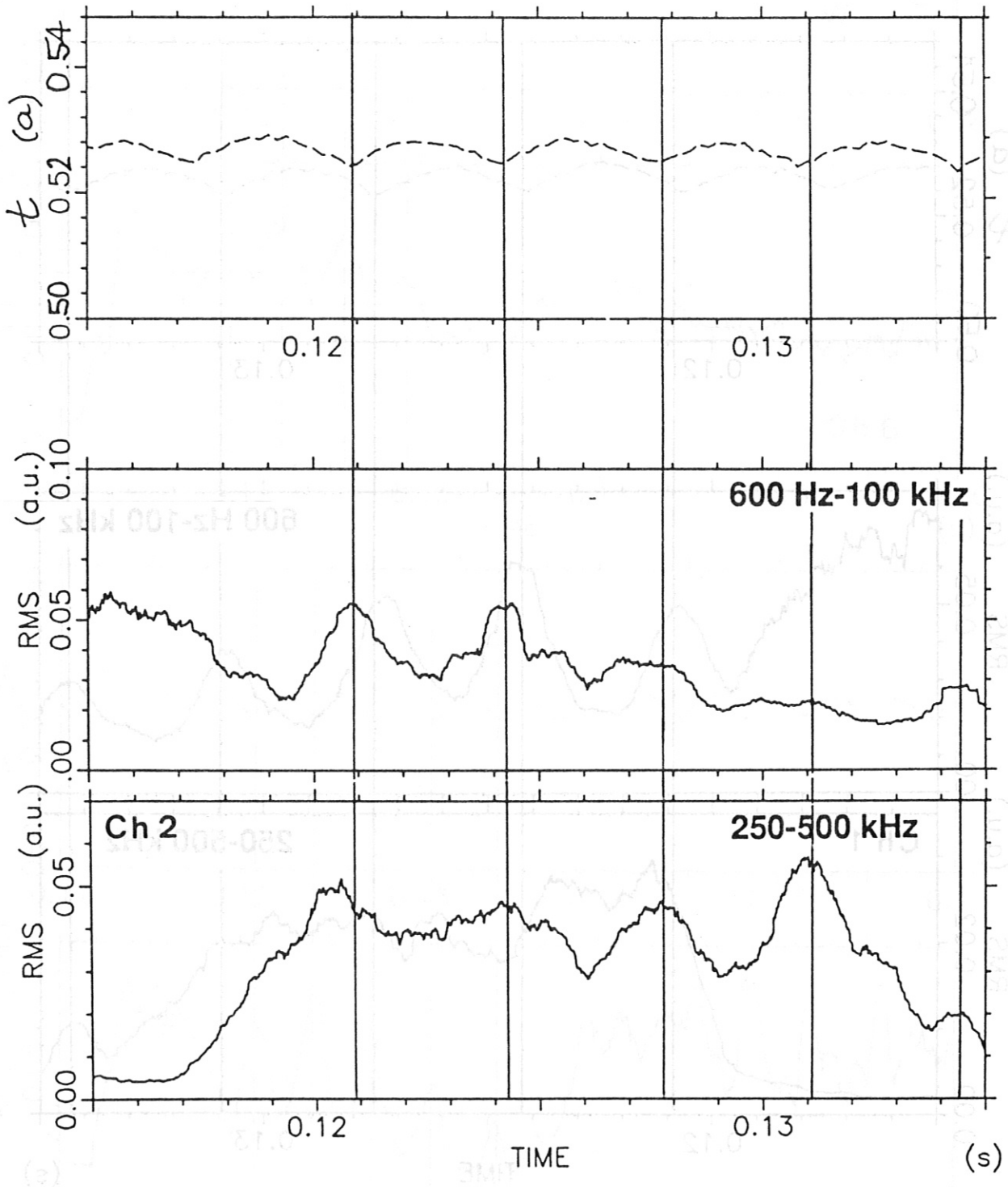

Fig.11. Different behaviour of the modulation when the low and high frequency components of the density turbulence are selected. Channel 2, f = 55 GHz. Upper frame: low frequency components, 600 Hz - 100 kHz. Lower frame: high frequency components, 250 - 500 kHz.

ber) the high frequency components show some modulation too. The only way to generate this behaviour is through changes in the evolution of $\delta(t)$ due to changes in the density turbulence. A modulation in the power p_1 due to any cause should give the same degree of modulation for the components of all frequencies.

The second consideration is based on the plasma - antenna geometry. If the amplitude modulation of the reflectometer signal is due to changes in the distance between antenna and the reflecting layer, big displacements of the cutoff layer are needed: a factor of 2 increase in the rms signal requires that the distance is reduced to 1/2, this implies 5 - 6 cm periodic displacement of the reflecting layer at 300 Hz. But this effect is not diagnosed otherwise.

A clear synchronization between iota and reflectometer signals exists exhibiting a phase jump as function of radial position.For the channels probing at radial positions r $\geq$ 0.11 m, iota minima correspond to increasing turbulence. The phase is opposed for r $\leq$ 0.11 m : high turbulence appears at the iota peaks.

A more exact analysis of the relative phase can be achieved by applying cross correlation techniques. Fig.12 gives the normalized cross correlation function of the iota, x(t), and rms reflectometer, y(t), signals. The evaluation has been done in the following way: first the low frequency components (below 50 Hz) have been removed from both signals. Then the normalized cross correlation function CN_{xy} is calculated by

$$CN_{xy} = \int_0^T x(t)y(t-\tau)dt / \sqrt{\int_0^T x^2(t)dt \int_0^T y^2(t)dt} \qquad (4)$$

The senoidal shape with high amplitude means good correlation. The signals are in phase for r$\leq$0.10 m (channel 6) and in opposed phase for r$\geq$0.11 m (channels 1 - 4). The phase jump appears just at the position where the stronger MHD activity is observed (figs.6 and 7).

The small advance of the reflectometer signal with respect to the iota signal for channels 1 and 2 is not seen when the comparison is made with the loop voltage instaed of iota. The iota edge value depends on the instantaneous value of the global plasma current, which has a small delay of the order of 10^{-4} s with respect to the loop voltage.

The whole picture is consistent with the idea that the whole iota profile is being modulated at 300 Hz (at least in the cold region) and that enhanced broadband density fluctuations are present at the rational iota surfaces: being iota at the edge 0.525, the turbulence increases when iota decreases because iota approximates 0.5 from above. Moving to more internal radii, the shear makes iota to descend and the "inversion point" $\iota = 0.5$ is crossed. For deeper positions the turbulence increases with increasing local iota since 0.5 is approximated from below.

In the former WENDELSTEIN VII-A machine, the correlation between density fluctuations and the edge iota value was observed as a global effect by microwave scattering [15]. Strong fluctuations where correlated to rational values of the edge iota. In contrast the observation presented here is a local increase of the turbulence at the position of a rational

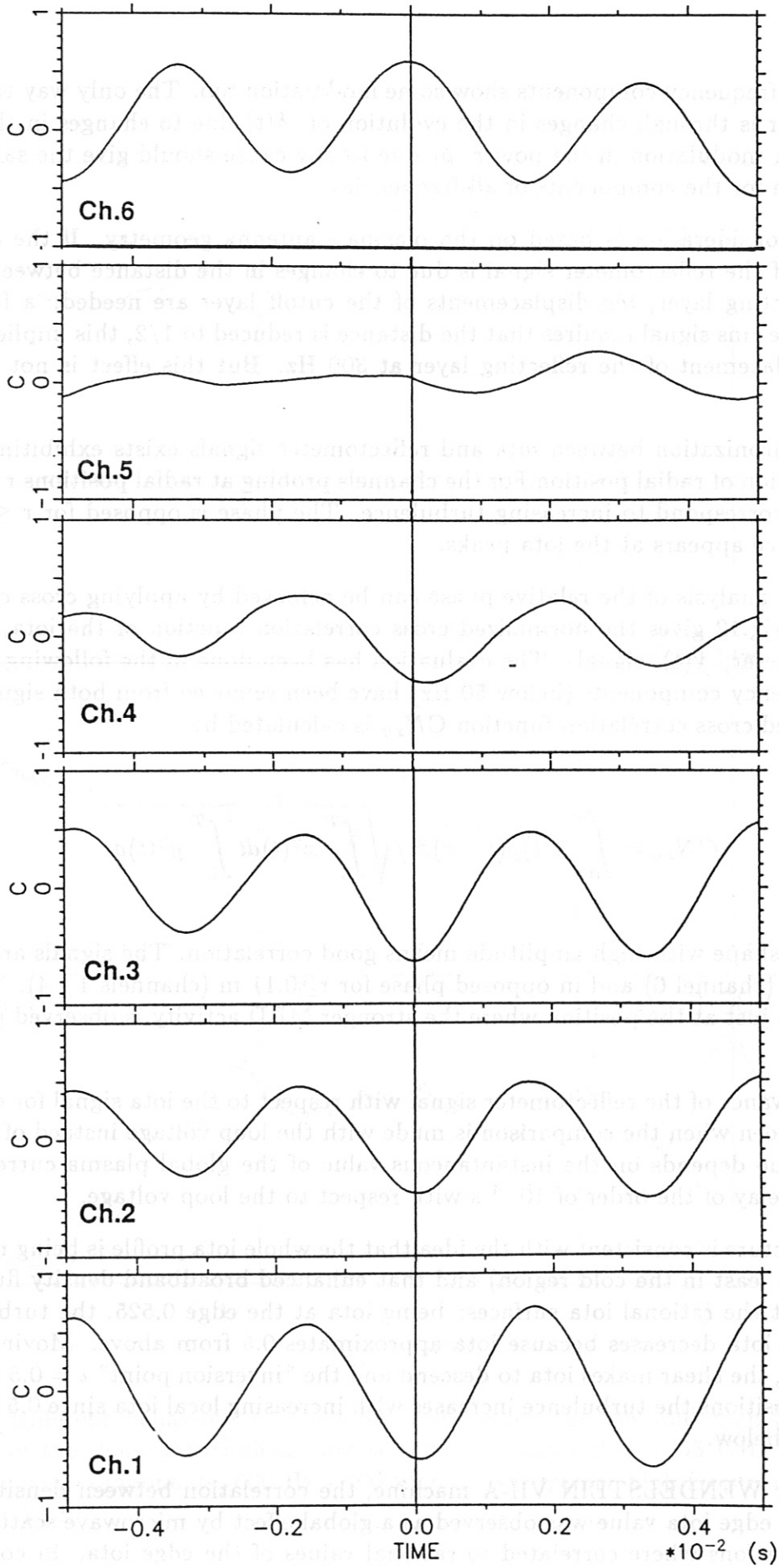

Fig.12. Normalized cross correlation function of the rms reflectometer and iota signals for different frequency channels. Channel 6 is in phase with iota, channels 1 to 4 are in opposed phase. The time interval of the cross correlation is 0.11 to 0.14 s.

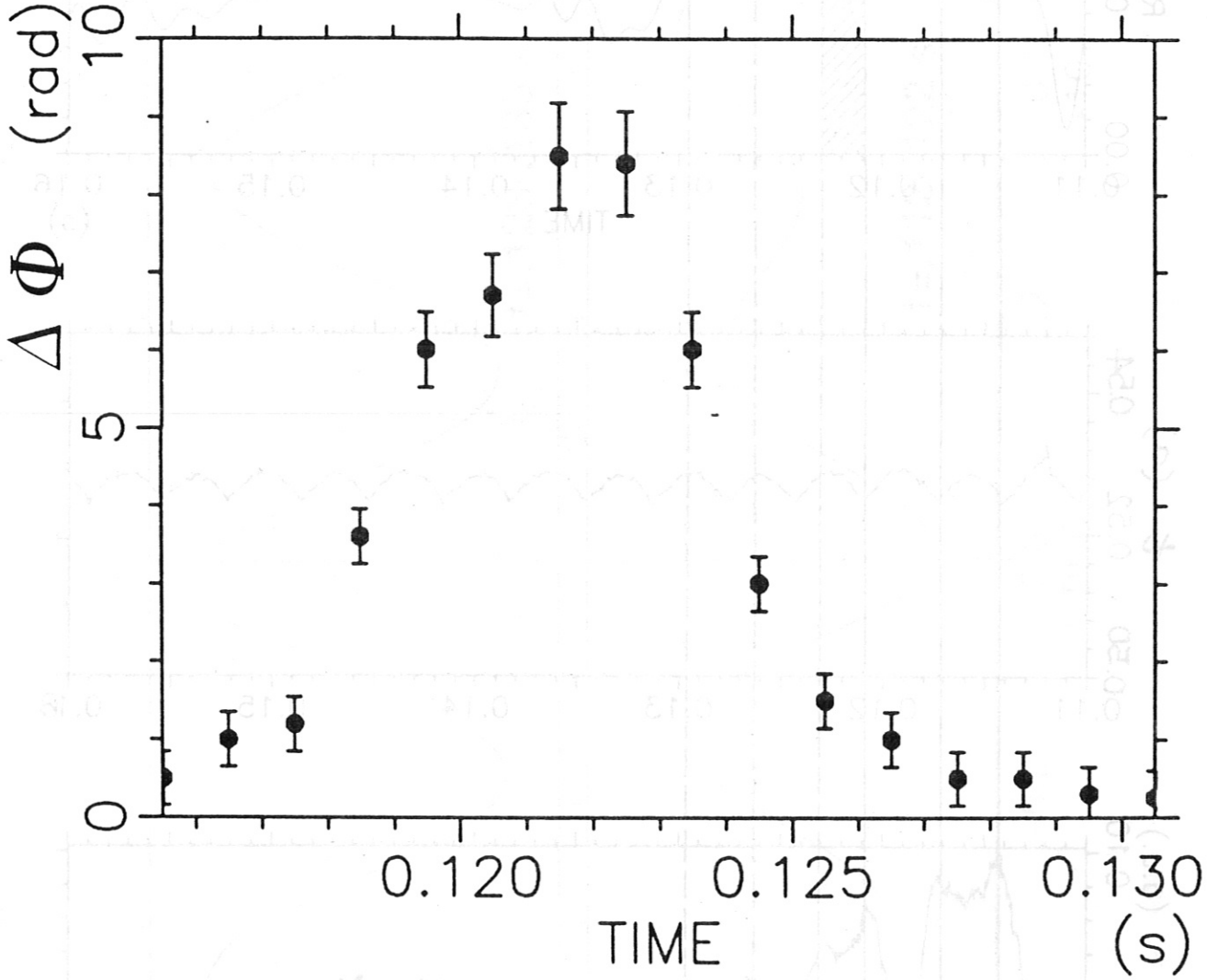

Fig.13. Time evolution of the phase oscillation amplitude $\Delta\Phi$ for channel 5, f = 68 GHz.

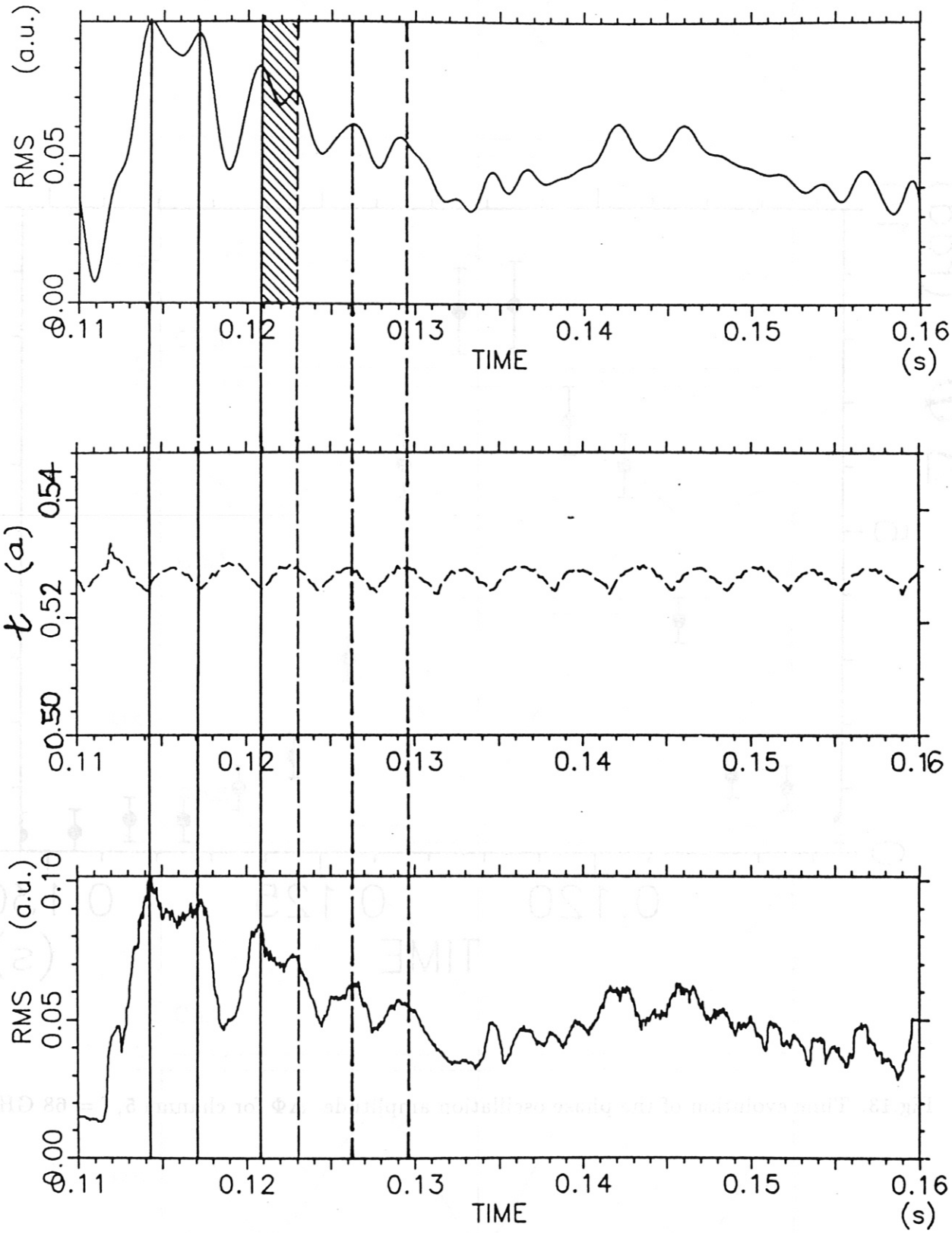

Fig.14. Time evolution of iota and channel 5 reflectometer signal. The phase change around t = 0.120 to 0.123 s can be seen directely. To emphazize the effect, rms signal has been smoothed with 1.7 ms time constant (upper frame).

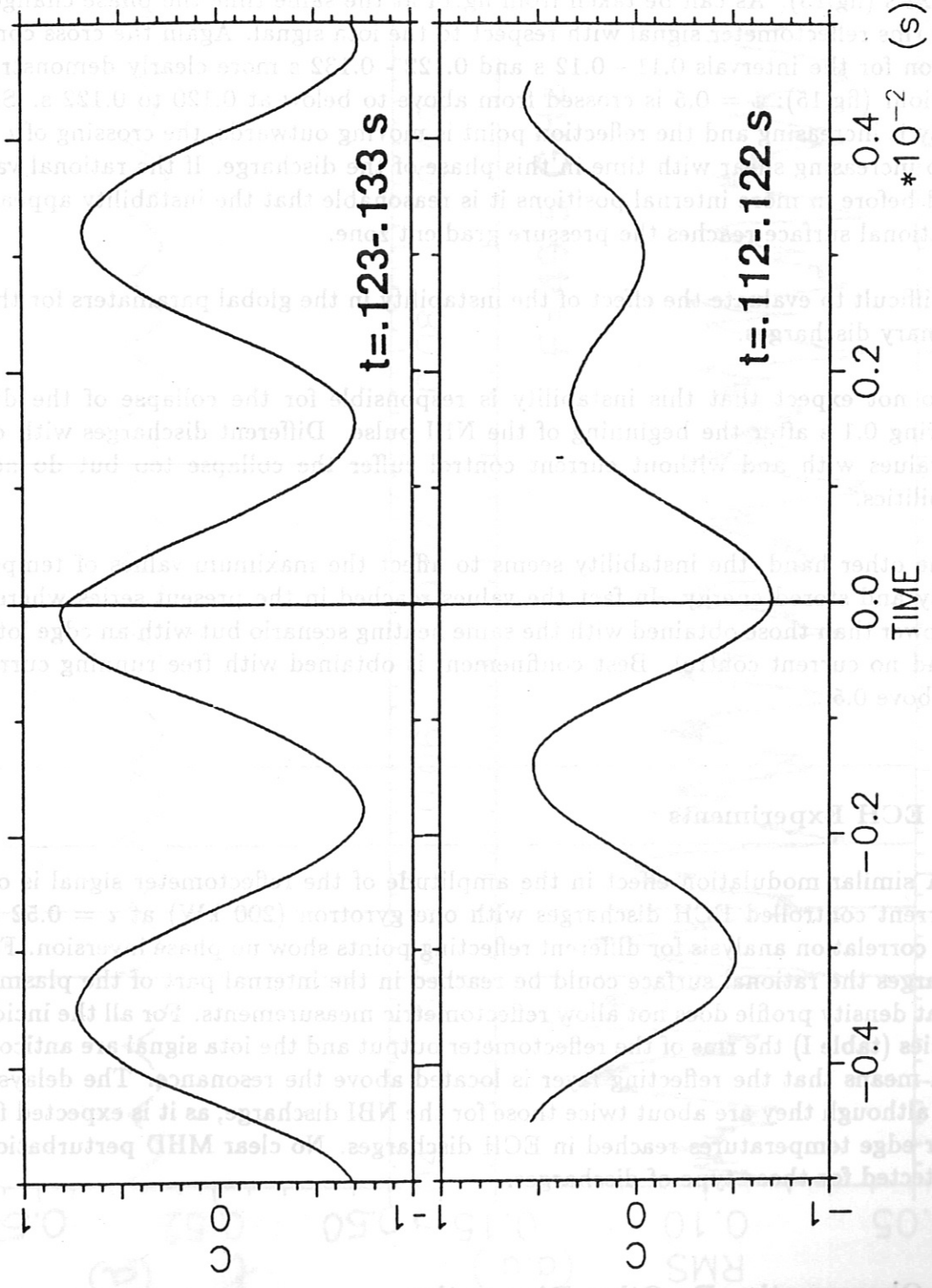

Fig.15. Cross correlation of iota and channel 5 reflectometer signal in the time interval 0.112 to 0.122 s (lower frame) and 0.123 to 0.133 s (upper frame). The phase jump can be seen.

surface.

From the temporal behaviour of the 68 GHz reflectometer channel the time can be determined at which the critical value is crossed. The maximum of MHD activity is reached at 0.122 s (fig.13). As can be taken from fig.14 at the same time the phase change occurs of the rms reflectometer signal with respect to the iota signal. Again the cross correlation function for the intervals 0.11 - 0.12 s and 0.122 - 0.132 s more clearly demonstrates the behaviour (fig.15): $\iota = 0.5$ is crossed from above to below at 0.120 to 0.122 s. Since the density is increasing and the reflection point is moving outwards, the crossing of $\iota = 0.5$ is due to increasing shear with time in this phase of the discharge. If the rational value was placed before in more internal positions it is reasonable that the instability appears when the rational surface reaches the pressure gradient zone.

It is difficult to evaluate the effect of the instability in the global paramaters for these non stationary discharges.

We do not expect that this instability is responsible for the collapse of the discharge occurring 0.1 s after the beginning of the NBI pulse. Different discharges with different iota values with and without current control suffer the collapse too but do not show instabilities.

On the other hand, the instability seems to affect the maximum values of temperature, density and stored energy. In fact the values reached in the present series where 50 per cent lower than those obtained with the same heating scenario but with an edge iota below 0.5 and no current control. Best confinement is obtained with free running current and iota above 0.5.

4.1.3 ECH Experiments

A similar modulation effect in the amplitude of the reflectometer signal is observed in current controlled ECH discharges with one gyrotron (200 kW) at $\iota = 0.52$ (fig.16). Cross correlation analysis for different reflecting points show no phase inversion. For those discharges the rational surface could be reached in the internal part of the plasma where the flat density profile does not allow reflectometric measurements. For all the incident frequencies (table I) the rms of the reflectometer output and the iota signal are anticorrelated which means that the reflecting layer is located above the resonance. The delays remain small although they are about twice those for the NBI discharge, as it is expected from the higher edge temperatures reached in ECH discharges. No clear MHD perturbation could be detected for those type of discharges.

4.1.4 Oberservation By Other Diagnostics

The effects of the iota modulation are also seen by edge sensitive diagnostics:H_α and the outer channels of the ECE radiometer. An increase of the modulation amplitude when the edge iota approaches rational values has been observed.

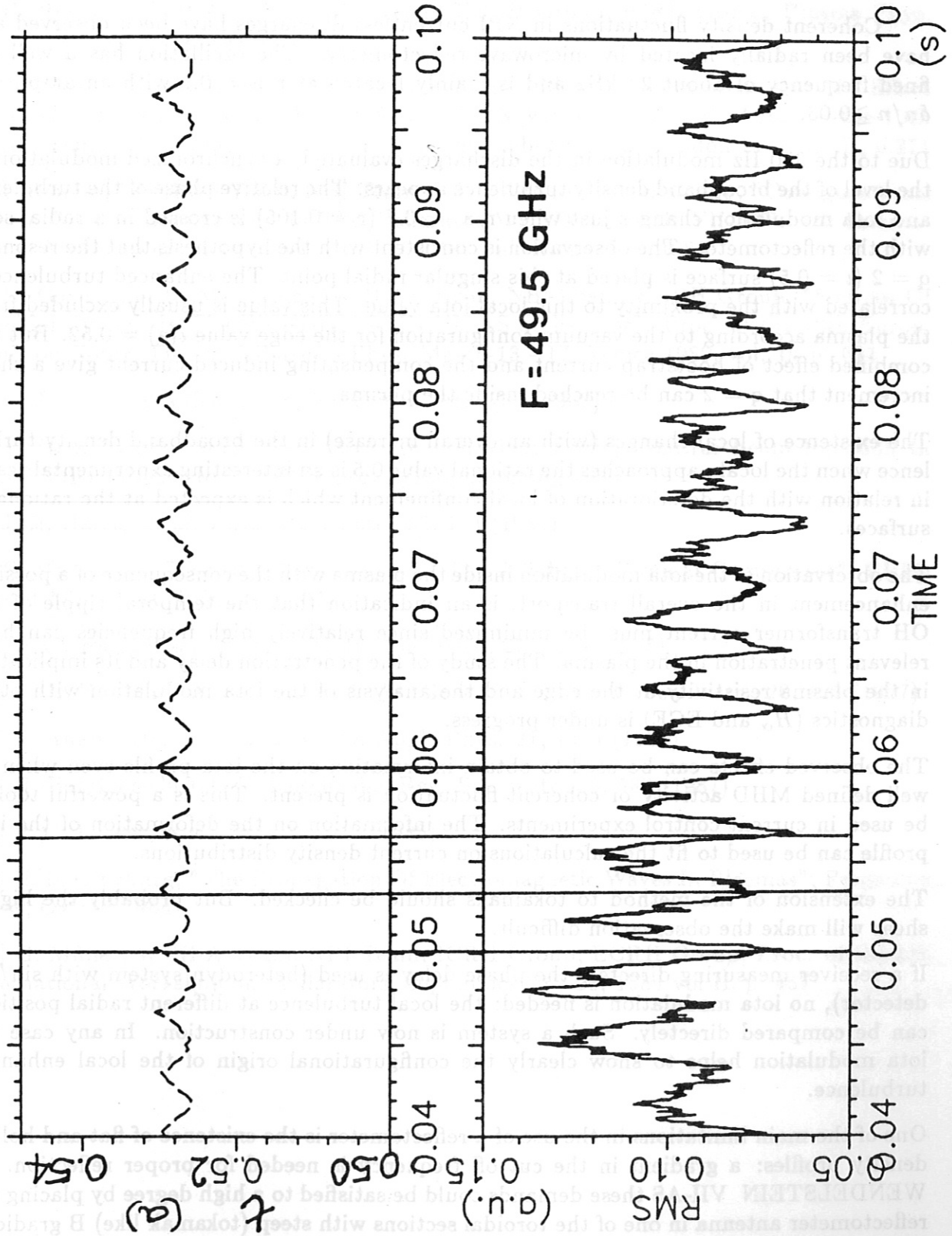

Fig.16. Time evolution of iota and rms reflectometer signals for an ECH discharge (200 kW) at $\iota(a) = 0.52$, probing frequency is 49.5 GHz corresponding to cut off density $8.5 \times 10^{18}\ m^{-3}$.

5. Summary and conclusions

Coherent density fluctuations in NBI currentless discharges have been observed and have been radially located by microwave reflectometry. The oscillation has a well defined frequency of about 22 kHz and is mainly located at r/a = 0.7 with an amplitude $\delta n/n \geq 0.03$.

Due to the 300 Hz modulation in the discharges evaluated, a synchronized modulation in the level of the broadband density turbulence appears. The relative phase of the turbulence and iota modulation changes just when r/a = 0.7 (r = 0.105) is crossed in a radial scan with the reflectometer. The observation is consistent with the hypothesis that the resonant q = 2 ($\iota = 0.5$) surface is placed at this singular radial point. The enhanced turbulence is correlated with the proximity to this local iota value. This value is usually excluded from the plasma according to the vacuum configuration for the edge value $\iota(a) = 0.52$. But the combined effect of bootstrap current and the compensating induced current give a shear increment that q = 2 can be reached inside the plasma.

The existence of local changes (with an overall increase) in the broadband density turbulence when the local ι approaches the rational value 0.5 is an interesting experimental result in relation with the deterioration of local confinement which is expected at the rational q surfaces.

The observation of the iota modulation inside the plasma with the consequence of a possible enhancement in the overall transport, is an indication that the temporal ripple of the OH transformer current must be minimized since relatively high frequencies can have relevant penetration in the plasma. The study of the penetration delay and its implication in the plasma resistivity at the edge and the analysis of the iota modulation with other diagnostics (H_α and ECE) is under progress.

The observed effects can be used to obtain information on the iota profile even when no well defined MHD activity or coherent fluctuation is present. This is a powerful tool to be used in current control experiments. The information on the deformation of the iota profile can be used to fit the calculations on current density distributions.

The extension of the method to tokamaks should be checked. But probably the higher shear will make the observation difficult.

If a receiver measuring directely the phase delay is used (heterodyn system with sin/cos detector), no iota modulation is needed: the local turbulence at different radial positions can be compared directely. Such a system is now under construction. In any case the iota modulation helps to show clearly the configurational origin of the local enhanced turbulence.

One of the main limitations in the use of a reflectometer is the existence of flat and hollow density profiles: a gradient in the cut off frequency is needed for proper reflection. In WENDELSTEIN VII-AS these demands could be satisfied to a high degree by placing the reflectometer antenna in one of the toroidal sections with steep (tokamak like) B gradient. The whole plasma radius up to the center would be accessible with the x-mode of the probing beam even for flat und moderately hollow density profiles. The potential of the ECE diagnostic to analyze temperature fluctuations with high radial resolution up to the plasma center should be used for comparison.

References

[1] H. Renner, WVII-AS Team, NBI Team, ECRH Group, ICRH Group, Plasma Phys. Contr. Fus. 31, 1579 (1989)

[2] WVII-A Team, NI Team, Pellet Injection Group, "Plasma Confinement And The Effect Of Rotational Transform In The WENDELSTEIN VII-A Stellarator". Proc. of the 10th Conf. Plasma Phys. and Contr. Nucl. Fus. September 12 - 19, London 1984, vol.II, p.371

[3] H.Renner, WVII-AS Team, NBI Team, ICRH Group, ECRH Group, "Configurational Effects On The Confinement In The Stellarator WENDELSTEIN VII-AS". 7th International Workshop on Stellarators, April 10 - 14, Oak Ridge, TN, 1989

[4] U. Gasparino, H. Maaßberg, WVII-AS Team, NBI Team, ECRH Group, "Sources Of Toroidal Current In The WENDELSTEIN VII-AS Stellarator". Proc. of the 16th Europ. Conf. on Contr. Fus. and Plasmas Phys. March 13 - 17, Venice 1989, vol. II, p. 631

[5] R. Jaenicke, WVII-A Team, Nucl. Fus., 28, 1737 (1988)

[6] WVII-A Team, "Mode And Sawtooth Behaviour During Neutral Beam Injection In The WVII-A Stellarator", IPP Report 2/250, Garching 1980.

[7] J. H. Harris, et al. Phys. Rev. Lett., 53, 114 (1984)

[8] E. Mazzucato, "Density Fluctuations In The Adiabatic Toroidal Compressor", PPPL Report Matt-1151, Princeton 1975

[9] TFR Group, Plasma Phys. Contr. Nuc. Fus., 27, 1299 (1985)

[10] A. E. Hubbard, A. E. Costley, C. W. Gowers, J. Phys. E: Sci. Instr., 20, 423 (1987)

[11] E. Anabitarte, et al. J. Phys. D: Appl. Phys. 21, 1384 (1988)

[12] H. Botollier-Curtet, G. Ichtchenko, Rev. Sci. Instr. 58, 539 (1987)

[13] P. C. Liewer, Nucl. Fus. 25, 543 (1985)

[14] U. L. Ginzburg, "The Propagation Of Electromagnetic Waves In Plasmas", Pergamon Press, Oxford 1964

[15] G. Müller, WVII-A Team, NBI Team, ICRH Group, ECRH Group, Proc. of the 5th International Workshop on Stellarators, September 24 - 28, 1984 vol II. p. 437